Arabian Journal of Chemistry (2022) **15**, 103720

King Saud University

Arabian Journal of Chemistry

www.ksu.edu.sa
www.sciencedirect.com

ORIGINAL ARTICLE

Astragalin identification in graviola pericarp indicates a possible participation in the anticancer activity of pericarp crude extracts: *In vitro* and *in silico* approaches

Xelha Araujo-Padilla [a], Eva Ramón-Gallegos [a], Francisco Díaz-Cedillo [b], Rafael Silva-Torres [c,*]

[a] *Laboratorio de Citopatología Ambiental, Departamento de Morfología, Escuela Nacional de Ciencias Biológicas del Instituto Politécnico Nacional, Ciudad de México 07738, Mexico*
[b] *Laboratorio de Síntesis 2, Departamento de Química Orgánica, Escuela Nacional de Ciencias Biológicas del Instituto Politécnico Nacional, Ciudad de México 11340, Mexico*
[c] *Laboratorio de anticonceptivos y antitumorales, Departamento de Farmacia, Escuela Nacional de Ciencias Biológicas del Instituto Politécnico Nacional, Ciudad de México 07738, Mexico*

Received 7 November 2021; accepted 19 January 2022
Available online 25 January 2022

KEYWORDS

Annona muricata;
Pericarp;
Cancerous cells;
kaempferol-3-O-glucoside;
Astragalin;
Targets prediction

Abstract Graviola, soursop, or guanabana (*Annona muricata* L.), is an ethnomedical fruit consumed to alleviate headache, diarrhea, diabetes, and cancer. Pericarp is the inedible part of graviola least studied in comparison to seeds and leaves, even thought, it contains the highest concentration of graviola total polyphenols. Anticancer effect of graviola pericarp has been demonstrated in crude extracts attributing the effect to acetogenins, however, crude extracts contain several active molecules. Thus, the present work aimed to fractionate and purify an ethanolic crude extract from graviola pericarp. Purified graviola pericarp fraction (PGPF) was evaluated on cancerous and non-cancerous cell lines, and then was identified by NMR, TOF-MS, and HPLC. Finally, an *in silico* analysis was performed to predict targets cancer-related of the molecule detected. Our results revealed IC_{50} values for cervix adenocarcinoma (HeLa), hepatocellular carcinoma (HepG2), triple-negative breast cancer (MDA-MB-231), and non-cancerous cell line (HaCaT) of 92.85 ± 1.23, 81.70 ± 1.09, 84.28 ± 1.08, and 170.2 ± 1.12 μg PGPF/mL, respectively. *In vitro* therapeutic indexes estimated as quantitative relationship between safety and efficacy of PGPF were 1.83, 2.08,

* Corresponding author.
E-mail addresses: xaraujop1500@alumno.ipn.mx (X. Araujo-Padilla), eramong@ipn.mx (E. Ramón-Gallegos), fdiazc@ipn.mx (F. Díaz-Cedillo), rafaelsilvatorres@hotmail.com (R. Silva-Torres).
Peer review under responsibility of King Saud University.

Production and hosting by Elsevier

https://doi.org/10.1016/j.arabjc.2022.103720

and 2.02 for HeLa, HepG2, and MDA-MB-231, respectively. The NMR analysis revealed astragalin (kaempferol-3-O-glucoside) in PGPF, a flavonoid not reported in graviola pericarp until now. Astragalin identity was confirmed by TOF-MS and HPLC. *In silico* results support previous reports about astragalin modulating proteins such as Bcl-2, CDK2, CDK4, MAPK and RAF1. Also, results suggest that astragalin may interact with other cancer-related proteins not associated previously with astragalin. In conclusion, astragalin may be contributing to the anticancer effect observed in graviola pericarp extracts.

1. Introduction

Graviola, soursop, or guanabana (*Annona muricata* L.), is an ethnomedical fruit distributed in the tropical regions of Central and South America, Western Africa, and Southeast Asia. Traditionally, inhabitants of these regions consume the fruit, leaves, bark, root, and seeds of graviola to alleviate headache, diarrhea, coughs, diabetes, and cancer (Coria-Téllez et al., 2018, Rady et al., 2018). The anticancer activity of *A. muricata* is mainly attributed to annonaceous acetogenins (Qazi et al., 2018, Rady et al., 2018, Yajid et al., 2018, Jacobo-Herrera et al., 2019, Errayes et al., 2020), even though, graviola contains active molecules such as alkaloids, phenols, and flavonoids (Prasad et al., 2019). Recently, the pericarp (peel, skin or husk) of fruits such as *Punica granatum* L. (Wong et al., 2021), *Garcinia mangostana* L. (Meylina et al., 2021), *Camellia japonica* L. (Cho et al., 2021), and *Capsicum annuum* L. (Chilczuk et al., 2020) has been identified as a source of bioactive molecules with anticancer properties. Analyses of graviola pericarp demonstrate acetogenins (Aguilar-Hernández et al., 2020) and the highest concentration of phenols, flavonoids (Adefegha et al., 2015), and total polyphenols (Aguilar-Hernández et al., 2019) compared with pulp, columella, and seeds. However, graviola pericarp is the inedible part least studied in comparison to seeds and leaves. Although, crude extracts from graviola pericarp exhibit antioxidant (Adefegha et al., 2015, Lee et al., 2016, Audu et al., 2019, Iyanda-Joel et al., 2019a, Orak et al., 2019), antiparasitic (Jaramillo et al., 2000), antibacterial (Karthikeyan et al., 2016, Iyanda-Joel et al., 2019b), antidiabetic, antihypertensive (Adefegha et al., 2015), and anticancer effects (Deep et al., 2016, Kuete et al., 2016, Robles et al., 2017, González-Pedroza et al., 2021, Jabir et al., 2021), the reported studies focus on crude extracts without purification and identification of molecules. Thus, the present work aimed to purify a fraction obtained from a crude extract of graviola pericarp. Purified graviola pericarp fraction (PGPF) was evaluated on cancerous and non-cancerous cell lines viability and PGPF identity was elucidated by Nuclear Magnetic Resonance (NMR), Time-of-Flight Mass (TOF-MS), and High-Performance Liquid Chromatography (HPLC). Finally, an *in silico* analysis was performed to predict targets cancer-related of the molecule detected.

2. Material and methods

2.1. Chemicals and cell lines

All reagents and solvents were analytical grade purchased from Sigma-Aldrich (St. Louis, MO, USA) and Merck KGaA (Darmstadt, HE, DEU). Cell culture reagents such as Dulbecco's modified Eagle's medium (DMEM), fetal bovine serum (FBS), and penicillin–streptomycin antibiotics were acquired from GIBCO (Grand Island, NY, USA), while MTT (3-(4,5-dimethylthiazol-2-yl)-2,5-diphenyltetrazolium bromide) reduction reagent was purchased from Sigma-Aldrich (St. Louis, MO, USA). Cervix adenocarcinoma (HeLa), hepatocellular carcinoma (HepG2), and triple-negative breast cancer (MDA-MB-231) cell lines were obtained from American Type Culture Collection (ATCC; Manassas, VA, USA), while non-cancerous immortalized keratinocytes (HaCaT) cell line was kindly provided by Dr. Mario Eugenio Cancino Díaz (Laboratorio de Inmunidad Innata, Departamento de Inmunología, Escuela Nacional de Ciencias Biológicas del Instituto Politécnico Nacional, México).

2.2. Graviola pericarp crude extract and phytochemical identification

Graviola fruit collected from Colima Mexico in February 2017 was identified as *Annona muricata* by the Botany Department (Escuela Nacional de Ciencias Biológicas del Instituto Politécnico Nacional). First, the fresh fruit was washed and peeled, and then the pericarp was fragmented and weighed. Pericarp crude extract was prepared by mixing ethanol (96 %, 3 L) and graviola pericarp (2.314 kg) for five days at room temperature. Solvent was removed under reduced pressure at 40 °C and secondary metabolites were identified in the crude extract by qualitative phytochemical screening tests as Dominguez described (1973). Coumarins, tannins, and quinones were detected by Erlich, jelly reagent, and ammonium hydroxide tests, respectively. Flavonoids were identified by Shinoda reagent and sodium hydroxide, while alkaloids were recognized by silicotungstic acid, Dragendorff method, and Mayer test.

2.3. Purified graviola pericarp fraction (PGPF)

Pericarp crude extract (42 g) was separated in a silica gel column with methanol-acetone (4:1). Fraction 5–8 was purified by preparative thin layer chromatography in silica gel 60 F_{254} plates eluting with methanol-acetone (4:1) and visualizing with UV light. Then, PGPF was evaluated on cancerous and non-cancerous cell viability, and PGPF identity was elucidated by NMR, TOF-MS, and HPLC.

2.4. Cell viability

The PGPF effect on cell viability of cancerous (HeLa, HepG2, and MDA-MB-231) and non-cancerous (HaCaT) cell lines was determined by MTT assay. Cells were grown and maintained as monolayer culture in DMEM supplemented with FBS (10 %), penicillin (100 U/mL), and streptomycin (100 µg/mL) at standard conditions in a humidified incubator (37 °C and 5 % CO_2). The PGPF was prepared in serum-free DMEM (5 mg PGPF/mL) and then sterilized by a syringe driven filter (0.22 µm pore size). Cells were seeded in 96-well culture plates

at $6x10^3$ cells/well and incubated 24 h in 0, 5, 50, 100, 150, 200, 250, and 500 μg PGPF/mL in triplicate. The PGPF was removed, and cells were incubated 3 h in MTT solution (0.1 mg/mL). Finally, MTT was discarded, and formazan crystals were dissolved with isopropanol (pH = 4). Wells absorbances (Abs) were measured at 595 nm in an ELISA ELx808 reader (BioTek, Winooski, VT, USA), and data were used to calculate cell viability (%) for each cell line by the following formula:

$$\text{Cell viability (\%)} = (\text{Abs}_{595} \text{ of PGPF treated cells}/\text{Abs}_{595} \text{ control cells})100$$

2.5. Statistical analysis

Cell viabilities from three independent experiments were analyzed by two-way analysis of variance (ANOVA) followed by Bonferroni *post hoc* test. The mean ± standard deviation (SD) was plotted for each cell line, and $p \leq 0.05$ was considered as statistically significant. Statistical analysis and graphs were performed in GraphPad Prism 5 (GraphPad Software Inc.).

2.6. Half maximal inhibitory concentration (IC_{50}) and in vitro therapeutic index

The IC_{50} of PGPF for each cell line was determined in GraphPad Prism 5. Cell viabilities from triplicate measures were normalized, and PGPF concentrations were transformed to logarithmic scale. Then, non-linear regression was performed to estimate the IC_{50} for each cell line. The IC_{50} ± SD, as well as the R^2 value were reported. On the other hand, the *in vitro* therapeutic indexes for cancer cell lines were estimated by the following formula as González-Pedroza (2021) described.

$$\textit{In vitro} \text{ therapeutic index} = IC_{50} \text{ non-cancerous cell line}/IC_{50} \text{ cancerous cell line}$$

2.7. Nuclear magnetic resonance (NMR), time-of-flight mass spectra (TOF-MS) and high-performance liquid chromatography (HPLC)

The PGPF was identified by ^1H and ^{13}C NMR. Tetradeuteromethanol (CD_3OD) was used as solvent, and trimethylsilane (TMS) was the internal standard. Spectra were recorded on Varian Mercury-300 NMR spectrometer (300 MHz and 75.4 MHz) (Varian Inc., Palo Alto, CA, USA), and data were compared with literature and an astragalin standard. Molecule identity was confirmed by TOF-MS and purity was evaluated by HPLC, the experimental conditions are described in the supplementary section. Molecule structure was drawn in ACD/ChemSketh (Freeware) version 2019.2.2.

2.8. In silico analyses

2.8.1. Targets prediction and protein–protein interaction (PPI) network

Astragalin 2D structure in SDF format was downloaded from PubChem database (https://pubchem.ncbi.nlm.nih.gov/) as Compound ID: 5282102. Astragalin targets prediction was performed by inverse docking in ACID web server (Auto *in silico* Consensus Inverse Docking, http://chemyang.ccnu.edu.cn/ccb/server/ACID/index.php/home/index), selecting Vina, PSO, LeDock, and PLANTS as docking software. The consensus inverse docking program contains 809 approved targets and it evaluates the binding affinity between astragalin and each target in database, outputting top potential targets and corresponding energy terms. ACID results were ordered from lowest to highest energy bind (ΔEbind = kcal/mol). Target names and their origin organism were searched in UniProt data base (https://www.uniprot.org). The first 150 targets from *Homo sapiens* were uploaded to STRING (Search Tool for the Retrieval of Interacting Genes/Proteins, https://string-db.org/) and a protein–protein interaction (PPI) network was determined. The STRING settings were selected as default: full STRING network, edges indicate evidence, all active interaction sources, medium confidence (0.4) for interaction score, non-maximum number of interactions to show, and interactive svg display mode. The STRING server presents an enrichment analysis of gene ontologies, pathways and domains that shows proteins grouped by their functional description. In the enrichment analysis proteins related with "Cancer", "Pathways in cancer", "Breast cancer pathway", and "Cervical carcinoma cell" were selected from the DISEASES (DOID:162), KEGG Pathways (hsa05200), WikiPathways (WP4262), and TISSUES (BTO:0000180), respectively.

2.8.2. Statistical data

The web server STRING estimated and provided statistical data of the inferred PPI network. Number of edges expected, and *p*-value of PPI enrichment were determined. Also, functional enrichments presented a false discovery rate by the *p*-values corrected from multiple testing within each category using the Benjamini-Hochberg procedure.

3. Results and discussion

3.1. Graviola pericarp crude extract, phytochemical identification, and fraction purification

In this study, we obtained 52.8 g of brown and viscous ethanolic crude extract from 2.314 kg of graviola pericarp. Crude extract evaluation by qualitative phytochemical screening tests revealed flavonoids, tannins, coumarins, alkaloids, and quinones in agreement with previous reports of ethanolic extracts from graviola pericarp analyzed by qualitative methods (Iyanda-Joel et al., 2019a, Iyanda-Joel et al., 2019b). Reports of crude extracts from graviola pericarp demonstrate anticancer properties attributed mainly to acetogenins (Deep et al., 2016), albeit crude extracts contain phytochemicals related to anticancer activity such as flavonoids (Kubczak et al., 2021), tannins (El Omari et al., 2021), coumarins, alkaloids (Huang et al., 2017), and quinones (Verrax et al., 2011). Moreover, these studies focus on evaluating crude extracts without purifying or identifying the molecules involved. Thus, we procured a PGPF to evaluate its effect on cancerous and non-cancerous cells. After fractionating and purifying 42 g of ethanolic crude extract we obtained 1.2 g of yellow PGPF (total yield of 28.57 mg/g extract).

3.2. Effect of PGPF on cancerous and non-cancerous cell viability

The Fig. 1 shows the viability of cancerous HeLa, HepG2, and MDA-MB-231 cell lines and non-cancerous HaCaT cells after

24 h incubation with PGPF. The PGPF reduced more than 90% the cell viability in cancerous and non-cancerous cell lines exposed to the highest concentrations (250 and 500 µg PGPF/mL). While at 50, 100, 150, and 200 µg PGPF/mL cell viability was decreased depending on cell lines; cancerous cells were significantly more affected than non-cancerous cells. The IC_{50} of PGPF was determined (Table 1) and cell lines sensitivity to PGPF was in the following order: HepG2 > MDA-MB-231 > HeLa > HaCaT. Subsequently, the *in vitro* therapeutic index was estimated for each cancerous cell line as a quantitative relationship between PGPF safety (IC_{50} on HaCaT) and efficacy (IC_{50} on HeLa, HepG2, and MDA-MB-231). Although, there is no universal therapeutic index value considered sufficient or required for a drug candidate a high therapeutic index is preferable, but a lower therapeutic index may be acceptable for treatment of life-threatening diseases that have limited treatment options (Muller and Milton 2012) such as cancer. The *in vitro* therapeutic indexes obtained were 1.83 (HeLa), 2.08 (HepG2), and 2.02 (MDA-MB-231), that are 10.8, 12.2, and 11.9-fold greater than the value (0.17) reported by Caba et al. (2011) for 5-fluorouracil estimated in the breast cancer MCF-7 cell line.

Table 1 The IC_{50} of PGPF and the *in vitro* therapeutic index.

Cell line	IC_{50} ± SD (µg PGPF/mL)	R^2	*In vitro* therapeutic index
HaCaT	170.2 ± 1.12	0.8748	
HeLa	92.85 ± 1.23	0.8888	1.83
HepG2	81.70 ± 1.09	0.9753	2.08
MDA-MB-231	84.28 ± 1.08	0.9759	2.02

IC_{50}, half maximal inhibitory concentration; SD, standard deviation; R^2, from non-linear regression.

3.3. PGPF identification by NMR, TOF-MS, and HPLC

The identity of PGPF was elucidated by NMR. Table 2 indicates the chemical shift values obtained from ^{1}H and ^{13}C spectrum. The NMR results unambiguously coincided with the spectrum values of kaempferol 3-O-glucoside, known as astragalin, previously identifyied in *Allium paradoxum* by Ghavam-Haghi and Sadeghi Dinani (2017). The TOF-MS results confirmed astragalin identity (Fig. S1), and estimations from HPLC indicated a purity of 97.3 % (Fig. S2). Kaempferol 3-O-glucoside (Fig. 2) is a flavonol common in nature (Calderon-Montano et al., 2011) identified in leaves from *Annona muricata* (Taiwo et al., 2019) and other species of Annonaceae family such as *A. mucosa* (Bicalho et al., 2012), *A. macroprophyllata* (Brindis et al., 2013), *A. cherimola* (Haykal et al., 2021), and *U. rufa* (Deepralard et al., 2009). However, there are not previous reports of astragalin in graviola pericarp. Interestingly, anticancer effect of astragalin on HeLa (Krauze-Baranowska et al., 2013, Zilla et al., 2014), HepG2 (Ahmed et al., 2016, Li et al., 2017, Hong et al., 2021), and MDA-MB-231 (Ahn et al., 2019) cell lines have been reported in agreement with our results (3.2 section). Also, protective effect of astragalin on HaCaT UV-irradiated was observed by Park et al. (2012). Thus, astragalin could be contributing to the anticancer properties reported for crude extracts of graviola pericarp. The identification of bioactive molecules in pericarp is relevant because it represents 20 % of the inedible graviola parts (Aguilar-Hernández et al., 2019), which are discarded as waste during the preparation of drinks, juices, jellies, jams, ice-creams, candies, and nectars in the food industry (Qazi et al., 2018). Therefore, bioactive molecules, such as astragalin, could be exploited at reduced

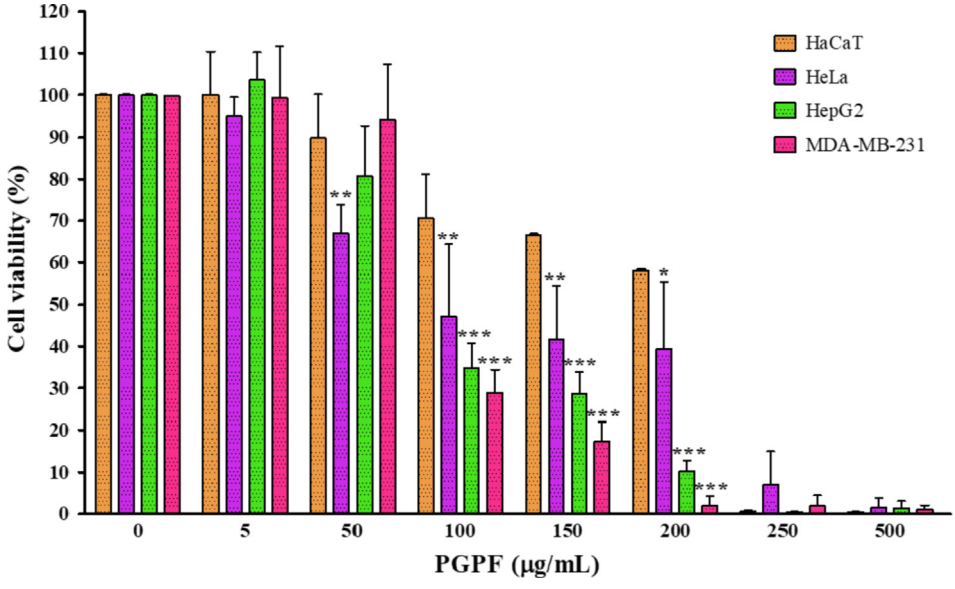

Fig. 1 Effect of purified graviola pericarp fraction (PGPF) on cancerous and non-cancerous cell viability. Columns represent the means ± standard deviation (SD) from three independent experiments performed in triplicate. Symbols *, **, and *** indicate $p \leq 0.05$, $p \leq 0.01$, and $p \leq 0.001$, respectively. Viability of cancerous cell lines HeLa, HepG2, and MDA-MB-231 was compared with non-cancerous HaCaT viability at the same PGPF concentration.

Table 2 Identification of PGPF by NMR. ^{1}H (300 MHz) and ^{13}C NMR (75.4 MHz) in CD_3OD solvent; spectroscopic data presented as chemical shifts (ppm), multiplicity, and *J* (Hz).

	PGPF		Standard		Literature*	
Carbon	$\delta^{1}H$	δ^{13} C	$\delta^{1}H$	δ^{13} C	δ ^{1}H ppm	$\delta^{13}C$
2		157.3		157.5		162.8
3		134.6		135.2		135.7
4		177.6		177.5		179.5
5		160.6		161.0		161.5
6	6.20 (1H, s)	99.4	6.21 (1H, s)	99.7	6.22 (1H, s)	99.7
7		164.6		164.8		165.9
8	6.40 (1H, s)	94.4	6.42 (1H, s)	94.7	6.41 (1H, s)	94.9
9		157.4		157.2		159.2
10		103.8		104.1		105.7
1′		122.2		122.6		122.6
2′, 6′	6.80 (2H, d, *J* = 8.6)	131.2	6.81 (2H, d, *J* = 8.5)	131.6	6.91 (2H, d, *J* = 8.5)	132.3
3′, 5′	8.00 (2H, d, *J* = 8.6)	115.6	8.05 (2H, d, *J* = 8.5)	116.0	8.07 (2H, d, *J* = 8.5)	116.1
4′		160.7		159.9		158.5
1″	5.30 (1H, d, *J* = 7.1)	102.5	5.29 (1H, d, *J* = 7.2)	102.7	5.26 (1H, d, *J* = 7.2)	103.9
2″	3.90 (1H, dd, *J* = 10.3, 3.9)	74.5	3.76 (1H, dd, *J* = 10.3, 3.8)	74.7	3.46 (1H, dd, *J* = 10.4, 3.6)	75.7
3″	4.03 (1H, m)	76.4	4.07 (1H, m)	76.8	3.37 (1H, m)	77.9
4″	3.10 (1H, m)	71.5	3.14 (1H, m)	71.4	3.24 (1H, m)	71.3
5″	3.30 (1H, m)	77.9	3.51(1H, m)	77.4	3.56 (1H, m)	78.4
6″	3.40 (2H, d, *J* = 11.2)	62.2	3.6 (2H, d, *J* = 11.3)	62.5	3.70 (2H, d, *J* = 11.5)	62.6

* NMR of astragalin reported by Ghavam-Haghi and Sadeghi Dinani (2017).

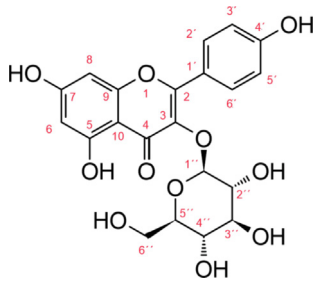

Fig. 2 Astragalin identified in PGPF.

costs by sustainable utilization of agri-food wastes (Ben-Othman et al., 2020).

3.4. In silico analyses

3.4.1. Astragalin targets prediction and interaction network

Astragalin exhibits various pharmacological properties, including anti-inflammatory, antioxidant, neurological, cardioprotective, antidiabetic, and anticancer effects (Peng et al., 2020). However, investigations are still mandatory to fully understand the mechanisms of action by which astragalin acts (Riaz et al., 2018). The anticancer effect of astragalin has been related with apoptosis induction. Hong et al. (2021), Wang et al. (2021), Xu et al. (2021), Yang et al. (2021), and You et al. (2017) suggest that astragalin induces apoptosis by modulation of Bcl-2 and Bax in liver, gastric, lung, colon, and melanoma cancers, respectively. Interestingly, apoptosis regulator Bcl-2 protein (Uniprot ID P10415, PDB 4LXD) ranks fourteenth (ΔEbind = –32.99 kcal/mol) in the results of targets prediction from ACID web server (Table S1). Thus, our results confirm the possible interaction of astragalin with Bcl-2, that is supported by Pirvu et al. (2018) in a molecular docking study. On the other hand, Yang et al. (2021) observed that astragalin induces cell arrest by modulation of CDK2 and CDK4 in cancerous colon cells. Both, cyclin-dependent kinase 2 (CDK2, Uniprot ID P4941, PDB 4EK4) and cyclin-dependent kinase 4 (CDK4, Uniprot ID P11802, PDB code 2W96) were identified as astragalin targets in our results with ΔEbind values −30.76 and −28.02 kcal/mol, respectively. The 150 targets of astragalin obtained by inverse docking in ACID web server are described in Table S1. After uploading the astragalin targets to STRING web server, the PPI network showed in Fig. 3 was obtained. Nodes represent the proteins (150) and edges indicate the interactions between proteins (698), network stats estimated a *p*-value < 1.0e−16 since 337 edges were expected. Consequently, predicted targets present more interactions among themselves than a random set of 150 proteins from the genome. From all the targets evaluated in STRING, 32 % present functional enrichments related with cancer. The *p*-values of functional enrichments were < 0.001 (Table S2). Proteins related with cancer, pathways in cancer, breast cancer pathway, and cervical carcinoma cell were colored yellow, purple, red, and green in the PPI network, respectively (Fig. 3). A Venn diagram in Fig. 4 shows the relation among proteins grouped by description enrichments, MAP2K1 and RAF1 coincide with the four enrichments selected in STRING. Particularly, these proteins are components of the pathway RAS-MAPK considered a potential therapeutic target for cancer treatment (Santarpia et al., 2012). Cho et al. (2014) reported that astragalin ameliorated oxidative stress by modulating MAPK signaling in an asthma model, while Asaad et al. (2021) demonstrated the inhibition of Raf/MAPK pathway by astragalin in mice treated with paracetamol. Therefore, interactions of astragalin with the targets predicted in ACID web server have been suggested in previous reports, however, targets such as ALDH2, CYP19A1,

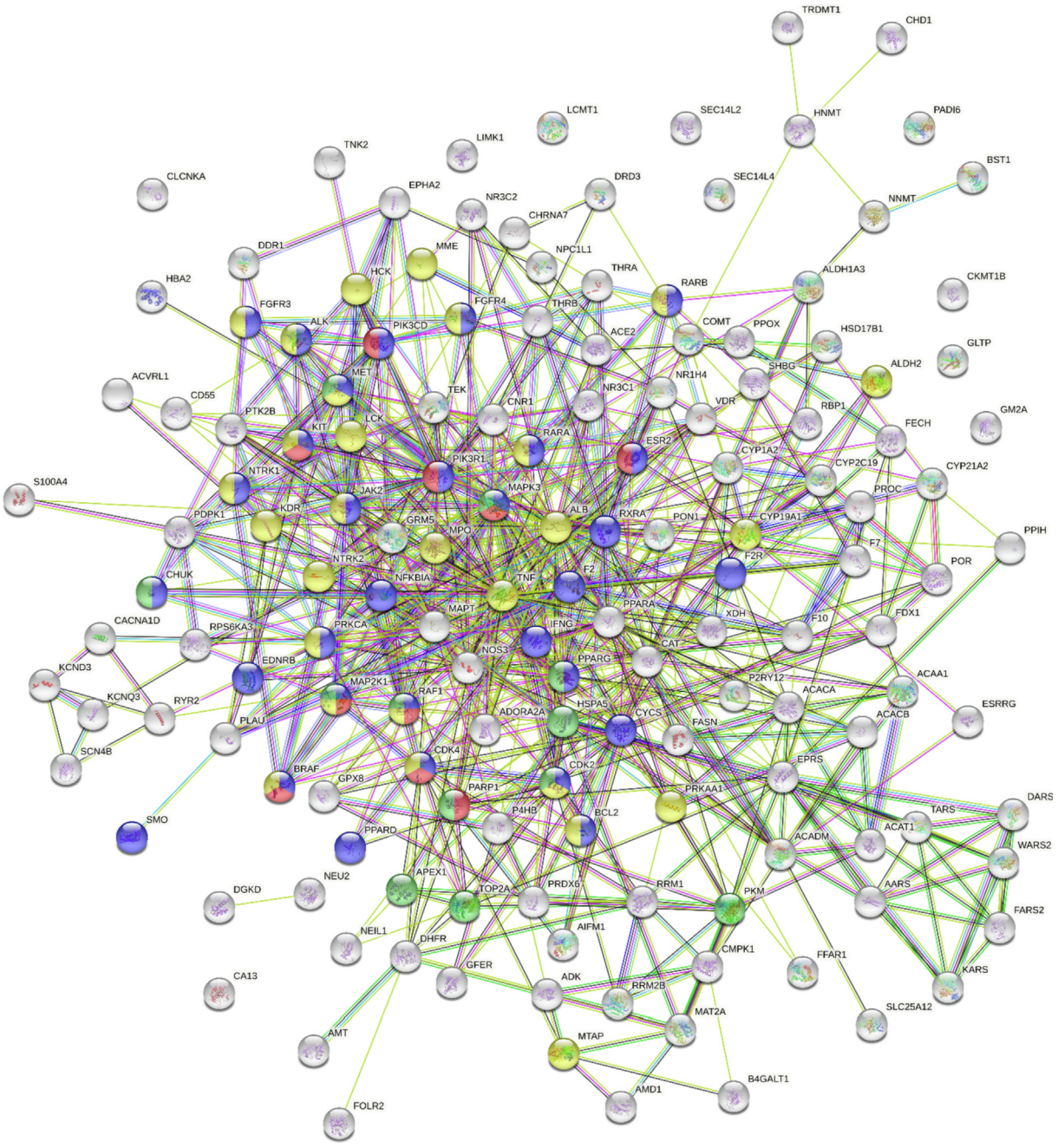

Fig. 3 Protein-protein interaction (PPI) network of astragalin predicted targets. Nodes represent proteins obtained from astragalin targets prediction, while edges indicate interactions between proteins. Nodes related with cancer, pathways in cancer, breast cancer pathway, and cervical carcinoma cell were colored yellow, purple, red, and green, respectively.

HCK, LCK, MME, MTAP, NTRK2, PRKAA1, MET, ALK, FGFR3, FGFR4, JAK2, NTRK1, RARA, RARB, PRKCA, PARP1, BRAF, KIT, APEX1, HSPA5, PKM, TOP2A, CHUK, CYCS, EDNRB, F2, F2R, NFKBIA, PPARD, RXRA, and SMO, remains unexplored in relation with astragalin. In conclusion, anticancer activity of astragalin has been widely studied but its interactions with cancer related proteins are poorly understood. Our *in silico* results suggest astragalin interactions with proteins previously not reported and results propose that astragalin contributes to the anticancer effect observed in crude extracts from graviola pericarp. Nevertheless, detailed experiments of the interactions are required.

4. Conclusion

Astragalin (kaempferol 3-O-glucoside) previously unidentified in graviola pericarp, was recognized in a PGPF obtained from a crude extract of graviola pericarp. The PGPF presented effect on cell viabilities of cancerous cell lines (HepG2, MDA-MB-231, and HeLa) at *in vitro* therapeutic indexes greater than 1.5. *In silico* targets prediction and

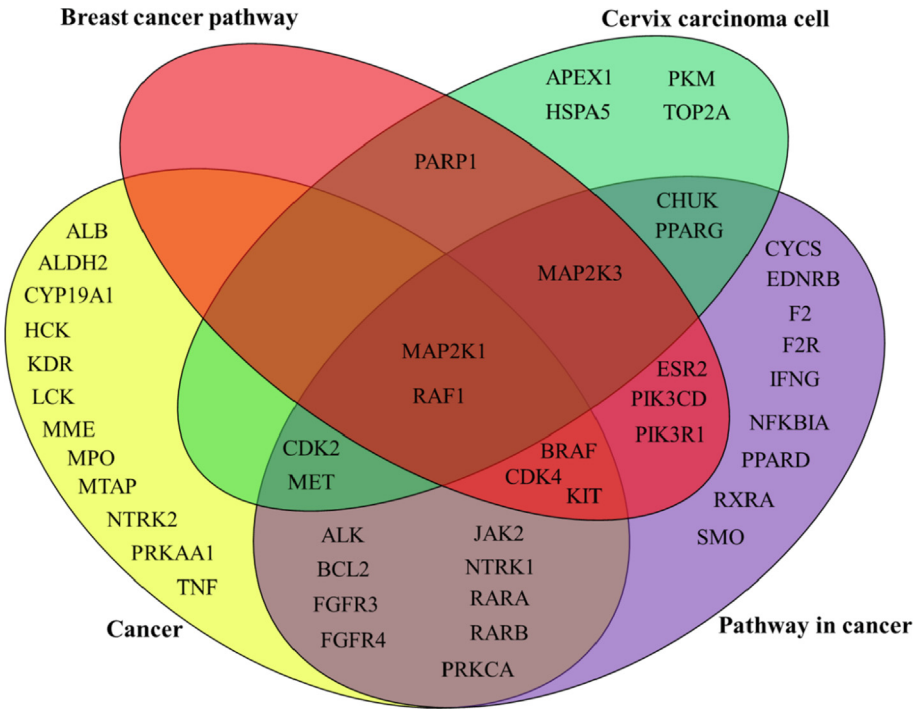

Fig. 4 Venn diagram from PPI network. Gene names of proteins grouped by the enrichment functions selected in STRING. Proteins are possible targets of astragalin elucidated by inverse docking in ACID web server.

analysis of PPI network suggest that astragalin interacts with proteins involved in cancer disease. Thus, astragalin may contribute to the anticancer effect observed in crude extracts from graviola pericarp.

Fund ing

This work was supported by Secretaría de Investigación y Posgrado del Instituto Politécnico Nacional (SIP-IPN, project number: 20171072), and by the Consejo Nacional de Ciencia y Tecnología (CONACyT, grant number: 419181).

Availability of data and material

Not applicable.

Code availability

Not applicable.

Authors' contributions

APX, performed *in vitro* and *in silico* assays, data analysis, diagrams elaboration, and the manuscript writing. RGE, planned and directed the *in vitro* and *in silico* analyses, reviewed data, and revised manuscript. DCF, performed molecule identification by NMR, data analysis, and revised the manuscript. STR, performed the extraction and purification, phytochemical identification, data analysis, and revised the manuscript.

Declaration of Competing Interest

The authors declare that they have no known competing financial interests or personal relationships that could have appeared to influence the work reported in this paper.

Acknowledgements

The authors are grateful to Secretaría de Investigación y Posgrado del Instituto Politécnico Nacional de México and to the Consejo Nacional de Ciencia y Tecnología for the support and scholarships awarded. Also, authors thank Dr. Mario Eugenio Cancino Díaz for donating HaCaT cell line.

Appendix A. Supplementary material

Supplementary data to this article can be found online at https://doi.org/10.1016/j.arabjc.2022.103720.

References

Adefegha, S.A., Oyeleye, S.I., Oboh, G., 2015. Distribution of phenolic contents, antidiabetic potentials, antihypertensive properties, and antioxidative effects of soursop (Annona muricata L.) fruit parts in vitro. Biochem. Res. Int. 2015. https://doi.org/10.1155/2015/347673.

Aguilar-Hernández, G., García-Magaña, M.L., Vivar-Vera, M., et al, 2019. Optimization of ultrasound-assisted extraction of phenolic compounds from *Annona muricata* by-products and pulp. Molecules 24. https://doi.org/10.3390/molecules24050904.

Aguilar-Hernández, G., Vivar-Vera, M.d.L.Á., García-Magaña, M.d.L., et al, 2020. Ultrasound-assisted extraction of total acetogenins

from the soursop fruit by response surface methodology. Molecules (Basel, Switzerland) 25, 1139. https://doi.org/10.3390/molecules25051139.

Ahmed, H., Moawad, A., Owis, A., et al, 2016. Flavonoids of *Calligonum polygonoides* and their cytotoxicity. Pharm. Biol. 54, 2119–2126. https://doi.org/10.3109/13880209.2016.1146778.

Ahn, S., Jung, H., Jung, Y., et al, 2019. Identification of the active components inhibiting the expression of matrix metallopeptidase-9 by TNFα in ethyl acetate extract of *Euphorbia humifusa* Willd. J. Appl. Biol. Chem. 62, 367–374. https://doi.org/10.3839/jabc.2019.051.

Asaad, G.F., Ibrahim Abdallah, H.M., Mohammed, H.S., et al, 2021. Hepatoprotective effect of kaempferol glycosides isolated from *Cedrela odorata* L. leaves in albino mice: involvement of Raf/MAPK pathway. Res. Pharm. Sci. 16, 370–380. https://doi.org/10.4103/1735-5362.319575.

Audu, S., Aremu, M., Beetseh, C., et al, 2019. Phytochemical screening, antioxidant activity and mineral composition of soursop (Annona muricata) pulp, peel and seed. FTSTJ https://doi.org/10.13140/RG.2.2.28043.03367.

Ben-Othman, S., Jõudu, I., Bhat, R., 2020. Bioactives from agri-food wastes: present insights and future challenges. Molecules (Basel, Switzerland) 25, 510. https://doi.org/10.3390/molecules25030510.

Bicalho, K., Reis, L.A., Graças, M.F., et al, 2012. Isolation and identification of flavonoids from *Annona mucosa*. Planta Med. 78. https://doi.org/10.1055/s-0032-1321251.

Brindis, F., González-Trujano, M.E., González-Andrade, M., et al, 2013. Aqueous extract of Annona macroprophyllata: a potential α-glucosidase inhibitor 591313-591313 Biomed. Res. Int. 2013. https://doi.org/10.1155/2013/591313.

Caba, O., Díaz-Gavilán, M., Rodríguez-Serrano, F., et al, 2011. Anticancer activity and cDNA microarray studies of a (RS)-1,2,3,5-tetrahydro-4,1-benzoxazepine-3-yl]-6-chloro-9H-purine, and an acyclic (RS)-O, N-acetalic 6-chloro-7H-purine. Eur. J. Med. Chem. 46, 3802–3809. https://doi.org/10.1016/j.ejmech.2011.05.047.

Calderon-Montano, J.M., Burgos-Moron, E., Lopez-Lazaro, C.P.-G. a.M., 2011. A review on the dietary flavonoid kaempferol. Mini Rev. Med. Chem. 11, 298–344. https://doi.org/10.2174/138955711795305335.

Coria-Téllez, A.V., Montalvo-Gónzalez, E., Yahia, E.M., et al, 2018. *Annona muricata*: a comprehensive review on its traditional medicinal uses, phytochemicals, pharmacological activities, mechanisms of action and toxicity. Arab. J. Chem. 11, 662–691. https://doi.org/10.1016/j.arabjc.2016.01.004.

Chilczuk, B., Marciniak, B., Stochmal, A., et al, 2020. Anticancer potential and capsianosides identification in lipophilic fraction of sweet pepper (*Capsicum annuum* L.). Molecules 25. https://doi.org/10.3390/molecules25133097.

Cho, E., Kim, J., Jeong, D.H., et al, 2021. Anticancer properties of dried-pericarp water extracts of *Camellia japonica* L. fermented with *Aspergillus oryzae* through regulation of IGFBP-2/mTOR pathway. Sci. 11, 21527. https://doi.org/10.1038/s41598-021-01127-3.

Cho, I.-H., Gong, J.-H., Kang, M.-K., et al, 2014. Astragalin inhibits airway eotaxin-1 induction and epithelial apoptosis through modulating oxidative stress-responsive MAPK signaling 122-122 BMC Pulm. Med. 14. https://doi.org/10.1186/1471-2466-14-122.

Deep, G., Kumar, R., Jain, A.K., et al, 2016. Graviola inhibits hypoxia-induced NADPH oxidase activity in prostate cancer cells reducing their proliferation and clonogenicity. Sci. 6, 23135. https://doi.org/10.1038/srep23135.

Deepralard, K., Kawanishi, K., Moriyasu, M., et al, 2009. Flavonoid glycosides from the leaves of *Uvaria rufa* with advanced glycation end-products inhibitory activity. Thai. J. Pharm. Sci. 33, 84–90.

Domínguez, X.A., 1973. Métodos de investigación fitoquímica. México.

El Omari, N., Bakha, M., Imtara, H., et al, 2021. Anticancer mechanisms of phytochemical compounds: focusing on epigenetic targets. Environ. Sci. Pollut. Res. Int. 28, 47869–47903. https://doi.org/10.1007/s11356-021-15594-8.

Errayes, A., Mohammed, W., Darwish, M., 2020. Review of phytochemical and medical applications of *Annona Muricata* fruits. J. Chem. Rev., 70–79 https://doi.org/10.33945/SAMI/JCR.2020.1.5.

Ghavam-Haghi, F., Sadeghi Dinani, M., 2017. Isolation and identification of Astragalin and 2-methoxy tyrosol from the bulbs of *Allium paradoxum*. J. HerbMed Pharmacol. 6, 114–118.

González-Pedroza, M.G., Argueta-Figueroa, L., García-Contreras, R., et al, 2021. Silver nanoparticles from *Annona muricata* peel and leaf extracts as a potential potent, biocompatible and low cost antitumor tool. Nanomaterials (Basel) 11. https://doi.org/10.3390/nano11051273.

Haykal, T., Younes, M., El Khoury, M., et al, 2021. The pro-apoptotic properties of a phytonutrient rich infusion of *A. cherimola* leaf extract on AML cells. Biomed. Pharmacother. 140, 111592. https://doi.org/10.1016/j.biopha.2021.111592.

Hong, Z., Lu, Y., Ran, C., et al, 2021. The bioactive ingredients in *Actinidia chinensis* Planch. Inhibit liver cancer by inducing apoptosis. J. Ethnopharmacol. 114553. https://doi.org/10.1016/j.jep.2021.114553.

Huang, L., Feng, Z.-L., Wang, Y.-T., et al, 2017. Anticancer carbazole alkaloids and coumarins from *Clausena plants*: a review. Chin. J. Nat. Med. 15, 881–888. https://doi.org/10.1016/S1875-5364(18)30003-7.

Iyanda-Joel, W.O., Ajetunmobi, O.B., Chinedu, S.N., et al, 2019a. Phytochemical, antioxidant and mitochondrial permeability transition studies on fruit-skin ethanol extract of *Annona muricata*. J. Toxicol. 2019, 7607031. https://doi.org/10.1155/2019/7607031.

Iyanda-Joel, W.O., Omonigbehin, E.A., Iweala, E.E.J., et al, 2019b. Antibacterial studies on fruit-skin and leaf extracts of *Annona muricata* in Ota, Nigeria. IOP Conf. Ser. Earth Environ. Sci. 331, 012029. https://doi.org/10.1088/1755-1315/331/1/012029.

Jabir, M.S., Saleh, Y.M., Sulaiman, G.M., et al, 2021. Green synthesis of silver nanoparticles using *Annona muricata* extract as an inducer of apoptosis in cancer cells and inhibitor for NLRP3 inflammasome via enhanced autophagy. Nanomaterials 11. https://doi.org/10.3390/nano11020384.

Jacobo-Herrera, N., Pérez-Plasencia, C., Castro-Torres, V.A., et al, 2019. Selective acetogenins and their potential as anticancer agents 783-783 Front. Pharmacol. 10. https://doi.org/10.3389/fphar.2019.00783.

Jaramillo, M.C., Arango, G.J., Gonzalez, M.C., et al, 2000. Cytotoxicity and antileishmanial activity of *Annona muricata* pericarp. Fitoterapia 71, 183–186. https://doi.org/10.1016/s0367-326x(99)00138-0.

Karthikeyan, K., Abitha, S., Kumar, V.G., 2016. Identification of bioactive constituents in peel, pulp of prickly custard apple (*Annona muricata*) and its antimicrobial activity. Int. J. Pharmacogn. Phytochem. 8, 1833–1838.

Krauze-Baranowska, M., Sowiński, P., Kawiak, A., et al, 2013. Flavonoids from *Pseudotsuga menziesii*. Z. Naturforsch. C: J. Biosci. 68, 87–96. https://doi.org/10.5560/znc.2013.68c0087.

Kubczak, M., Szustka, A., Rogalińska, M., 2021. Molecular targets of natural compounds with anti-cancer properties. Int. J. Mol. Sci. 22. https://doi.org/10.3390/ijms222413659.

Kuete, V., Dzotam, J.K., Voukeng, I.K., et al, 2016. Cytotoxicity of methanol extracts of Annona muricata, Passiflora edulis and nine other Cameroonian medicinal plants towards multi-factorial drug-resistant cancer cell lines 1666-1666 Springerplus 5. https://doi.org/10.1186/s40064-016-3361-4.

Lee, W.Z., Chang, S.K., Khoo, H.E., et al, 2016. Influence of different extraction conditions on antioxidant properties of soursop peel. Acta Sci. Pol. Technol. Aliment. 15, 419–428. https://doi.org/10.17306/j.afs.2016.4.40.

Li, W., Hao, J., Zhang, L., et al, 2017. Astragalin reduces hexokinase 2 through increasing miR-125b to inhibit the proliferation of hepatocellular carcinoma cells in vitro and in vivo. J. Agric. Food Chem. 65, 5961–5972. https://doi.org/10.1021/acs.jafc.7b02120.

Meylina, L., Muchtaridi, M., Joni, I.M., et al, 2021. Nanoformulations of α-mangostin for cancer drug delivery system. Pharmaceutics 13. https://doi.org/10.3390/pharmaceutics13121993.

Muller, P.Y., Milton, M.N., 2012. The determination and interpretation of the therapeutic index in drug development. Nat. Rev. Drug Discov. 11, 751–761. https://doi.org/10.1038/nrd3801.

Orak, H.H., Bahrisefit, I.S., Sabudak, T., 2019. Antioxidant activity of extracts of soursop (*Annona muricata* L.) leaves, fruit pulps, peels, and seeds. Polish J. Food Nutr. Sci. 69, 359–366. https://doi.org/10.31883/pjfns/112654.

Park, J.M., Cho, J.-K., Mok, J.Y., et al, 2012. Protective effect of astragalin and quercetin on ultraviolet (UV)-irradiated damage in HaCaT cells and Balb/c mice. J. Korean Soc. App. Biol. Chem. 55, 443–446. https://doi.org/10.1007/s13765-012-2072-y.

Peng, L., Gao, X., Nie, L., et al, 2020. Astragalin attenuates dextran sulfate sodium (DSS)-induced acute experimental colitis by alleviating gut microbiota dysbiosis and inhibiting NF-κB activation in mice. Front. Immunol. 11. https://doi.org/10.3389/fimmu.2020.02058.

Pirvu, L., Stefaniu, A., Neagu, G., et al, 2018. In Vitro cytotoxic and antiproliferative activity of *Cydonia oblonga* flower petals, leaf and fruit pellet ethanolic extracts. Docking simulation of the active flavonoids on anti-apoptotic protein Bcl-2. Open Chem. 16, 591–604. https://doi.org/10.1515/chem-2018-0062.

Prasad, S., Varsha, V., Devegowda, D., 2019. Anti-cancer properties of *Annona muricata* (L.): a review. Med. Plants – Int. J. Phytomed. Relat. Ind. 11, 123. https://doi.org/10.5958/0975-6892.2019.00016.9.

Qazi, A.K., Siddiqui, J.A., Jahan, R., et al, 2018. Emerging therapeutic potential of graviola and its constituents in cancers. Carcinogenesis 39, 522–533. https://doi.org/10.1093/carcin/bgy024.

Rady, I., Bloch, M.B., Chamcheu, R.N., et al, 2018. Anticancer properties of graviola (*Annona muricata*): a comprehensive mechanistic review. Oxid. Med. Cell Longev. 2018, 1826170. https://doi.org/10.1155/2018/1826170.

Riaz, A., Rasul, A., Hussain, G., et al, 2018. Astragalin: a bioactive phytochemical with potential therapeutic activities. Adv. Pharmacol. Sci. 2018, 9794625. https://doi.org/10.1155/2018/9794625.

Robles, J.F., Muñoz, K., Rivera, N., et al, 2017. Anti-proliferative properties of methanolic extracts of Annona muricata in colon, lung and skin cancer cell lines 807.805-807.805 FASEB J. 31. https://doi.org/10.1096/fasebj.31.1_supplement.807.5.

Santarpia, L., Lippman, S.M., El-Naggar, A.K., 2012. Targeting the MAPK-RAS-RAF signaling pathway in cancer therapy. Expert Opin. Ther. Targets 16, 103–119. https://doi.org/10.1517/14728222.2011.645805.

Taiwo, F., Oyedeji, O., Osundahunsi, M., 2019. Antimicrobial and antioxidant properties of kaempferol-3-O-glucoside and 1-(4-Hydroxyphenyl)-3-phenylpropan-1-one Isolated from the Leaves of *Annona muricata* (Linn.). J. Pharm. Res. Int. 1–13. https://doi.org/10.9734/jpri/2019/v26i330138.

Verrax, J., Beck, R., Dejeans, N., et al, 2011. Redox-active quinones and ascorbate: an innovative cancer therapy that exploits the vulnerability of cancer cells to oxidative stress. Anticancer Agents Med. Chem. 11, 213–221. https://doi.org/10.2174/187152011795255902.

Wang, Z., Lv, J., Li, X., et al, 2021. The flavonoid Astragalin shows anti-tumor activity and inhibits PI3K/AKT signaling in gastric cancer. Chem. Biol. Drug Des. https://doi.org/10.1111/cbdd.13933.

Wong, T.L., Strandberg, K.R., Croley, C.R., et al, 2021. Pomegranate bioactive constituents target multiple oncogenic and oncosuppressive signaling for cancer prevention and intervention. Semin. Cancer Biol. 73, 265–293. https://doi.org/10.1016/j.semcancer.2021.01.006.

Xu, G., Yu, B., Wang, R., et al, 2021. Astragalin flavonoid inhibits proliferation in human lung carcinoma cells mediated via induction of caspase-dependent intrinsic pathway, ROS production, cell migration and invasion inhibition and targeting JAK/STAT signalling pathway. Cell Mol. Biol. (Noisy-le-grand) 67, 44–49. https://doi.org/10.14715/cmb/2021.67.2.7.

Yajid, A.I., Ab Rahman, H.S., Wong, M.P.K., et al, 2018. Potential benefits of *Annona muricata* in combating cancer: a review. Malays J. Med. Sci. 25, 5–15. https://doi.org/10.21315/mjms2018.25.1.2.

Yang, M., Li, W.-Y., Xie, J., et al, 2021. Astragalin inhibits the proliferation and migration of human colon cancer HCT116 cells by regulating the NF-κB signaling pathway. Front. Pharmacol. 12, 639256. https://doi.org/10.3389/fphar.2021.639256.

You, O.H., Shin, E.A., Lee, H., et al, 2017. Apoptotic effect of astragalin in melanoma skin cancers via activation of caspases and inhibition of sry-related HMg-box gene 10. Phytother. Res. 31, 1614–1620. https://doi.org/10.1002/ptr.5895.

Zilla, M.K., Nayak, D., Amin, H., et al, 2014. 4′-Demethyl-deoxypodophyllotoxin glucoside isolated from *Podophyllum hexandrum* exhibits potential anticancer activities by altering Chk-2 signaling pathway in MCF-7 breast cancer cells. Chem. Biol. Interact. 224, 100–107. https://doi.org/10.1016/j.cbi.2014.09.022.